ChemComm

Electron doping of single-walled carbon nanotubes using pyridine-boryl radicals

Journal:	*ChemComm*
Manuscript ID	CC-COM-03-2021-001354.R1
Article Type:	Communication

COMMUNICATION

Electron doping of single-walled carbon nanotubes using pyridine-boryl radicals

Received 00th January 20xx,
Accepted 00th January 20xx

DOI: 10.1039/x0xx00000x

Naoki Tanaka,*[a,b] Aoi Hamasuna,[a] Takuto Uchida,[a] Ryohei Yamaguchi,[a] Taiki Ishii,[a] Aleksandar Staylkov[b] and Tsuyohiko Fujigaya*[a,b,c]

Pyridine-boryl (py-boryl) radicals serve as efficient electron-doping reagents for single-walled carbon nanotubes (SWCNTs). The doping mechanism comprises electron transfer from the py-boryl radical to the SWCNT. The formation of a stable py-boryl cation is essential for efficient doping; the captodative effect of the py-boryl cation is important to this process.

The chemical doping of single-walled carbon nanotubes (SWCNTs) using electron donor and acceptor molecules is a crucial step for controlling the frontier orbital energy gap of SWCNTs. This means that SWCNTs are a promising material for electronics applications such as thermoelectric conversion and thin-film transistors, due to their flexibility, stability and light weight.[1] Among all chemical dopants,[2] organic dopants containing hetero atoms are important materials as they permit fine controllability of the doping level; they also provide stability due to the flexibility of their structural design. In particular, dopant molecules containing elements from groups 15 to 17 (such as N, O, S and P) in their second and third periods can act as electron and hole dopants due to the electron-donating properties of the lone-pair electrons and the electronegativities of their heteroatoms, respectively. For example, tetracyanoquinodimethane,[3] carbazole[4] and poly(styrenesulfonate)[5] have been reported as hole dopants for SWCNTs, while poly(ethylenimine),[6] benzyl viologen[7] and triphenylphosphine[3] have been reported as electron dopants. Boron, a group 13 element in the second period, has been used as a hole dopant for SWCNTs based on its electron deficiency.[4,8]

For two decades, chemists have been developing boron compounds with electron-donating properties, such as boryl anions and radicals.[9,10] However, these compounds have not been used as electron dopants for SWCNTs, in part because of their lack of thermal and chemical stability, which is caused by their electron deficiency.

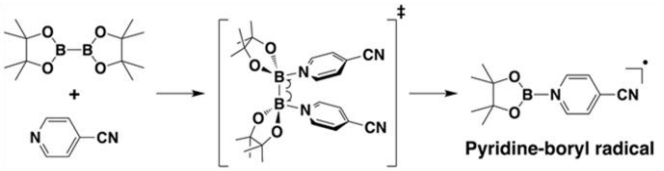

Fig. 1 Generation of 4-CNpy-boryl radical by a homolytic B–B bond cleavage of B_2pin_2 via coordination of 4-CNpy.

Wang et al. have recently predicted a presence of 4-cyanopyridine (4-CNpy)-boryl radical as the intermediate that was generated and stabilised by the coordination of 4-CNpy (Fig. 1).[11] They used theoretical calculations to clarify that pyridines with electron-withdrawing groups in the para-position offer stable radicals when coordinated to boron sources (the captodative effect).[12] Such electron-donating boryl radicals are of great interest regarding the electron doping of SWCNTs due to their high singly occupied molecular orbital (SOMO) levels. In fact, sulfoxides have been deoxygenated to sulfides and azo-compounds and quinones have been reduced under mild conditions using 4-CNpy-boryl radicals. These reactions have been achieved via coordination of substrates to the boron centre and single electron transfer.[11]

Here, we investigated the electron doping of SWCNTs using 4-CNpy-boryl radical, which can be easily prepared by reacting bis(pinacolate)diboron (B_2pin_2) with 4-CNpy as the boron source and ligand, respectively. This results in the homolytic cleaving of the B–B bond via cooperative coordination of 4-CNpy to the two boron atoms of B_2pin_2 (Figs. 1 and 2a).

Previously, we have reported that 2-(2-methoxyphenyl)-1,3-dimethyl-2,3-dihydro-1*H*-benzo[*d*]imidazole (*o*-MeO-DMBI) acts as an electron dopant via a neutral *o*-MeO-DMBI radical.[13] It was found that forming stable cations after doping was essential for stable electron doping. In 4-CNpy-boryl radical, formation of the cation after the electron transfer can be

[a] *Department of Applied Chemistry, Graduate School of Engineering, Kyushu University, 744 Motooka, Nishi-ku, Fukuoka 819-0395, Japan.*
[b] *International Institute for Carbon-Neutral Energy Research (WPI-I2CNER), Kyushu University, 744 Motooka, Nishi-ku, Fukuoka 819-0395, Japan*
[c] *Center for Molecular Systems (CMS), Kyushu University, 744 Motooka, Nishi-ku, Fukuoka 819-0395, Japan.*

† Electronic Supplementary Information (ESI) available: Experimental details, additional spectroscopic data, Seebeck Coefficient data and SEM images. See DOI: 10.1039/x0xx00000x

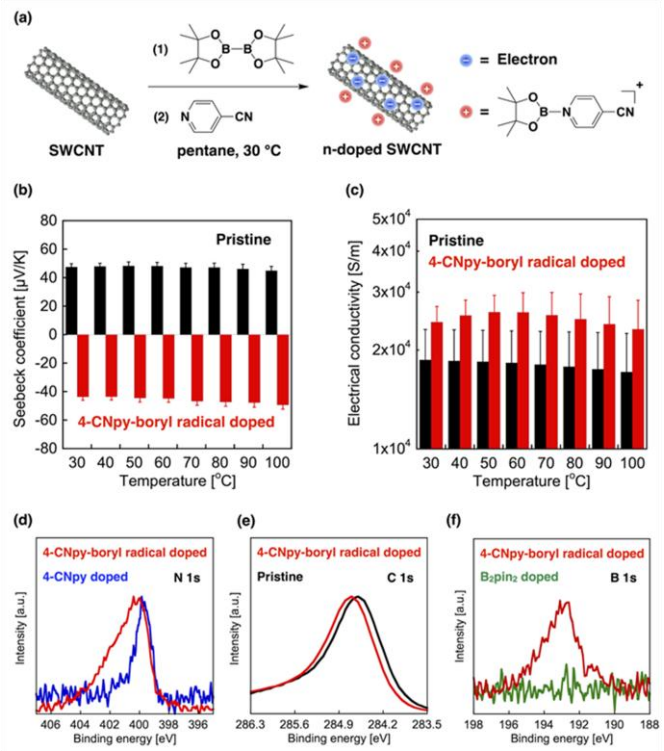

Fig. 2 (a) Electron doping of SWCNTs using a mixture of B_2pin_2 and 4-CNpy, and the formation of n-doped SWCNTs stabilised by the 4-CNpy-boryl cation. Temperature dependence of (b) Seebeck coefficient and (c) electrical conductivities of pristine SWCNT film (black) and SWCNT film doped with 4-CNpy-boryl radical (red). X-ray photoelectron spectroscopy (XPS) narrow scans of (d) N 1s, (e) C 1s and (f) B 1s of the n-doped SWCNT films (red line). Black line: pristine SWCNT film, blue line: SWCNT film using 4-CNpy and green line: SWCNT film using B_2pin_2.

expected owing to the delocalization in the pyridine ligands. Gao et al. recently reported that boron-nitrogen derivatives serve as electron dopants for SWCNTs.[14] However, they did not discuss the detailed mechanisms of electron transfer or cation formation. Here, we demonstrate that 4-CNpy-boryl radical serve as an efficient electron-doping reagent for SWCNTs and form the 4-CNpy-boryl cation after doping (Fig. 2a).

Prior to doping SWCNTs with 4-CNpy-boryl radical, we confirmed that a pentane solution of B_2pin_2 and 4-CNpy showed electron spin resonance (ESR) under nitrogen at room temperature (Fig. S1, ESI†), as has been previously reported.[11] The SWCNT films (15 μm in thickness) were immersed in the solution at 30 °C, after which the mixture was shaken for three hours (Fig. 2a). After drying the films, the temperature dependence of the Seebeck coefficient and the electrical conductivities of the films were measured under helium conditions (Fig. 2b). Positive and negative Seebeck coefficients indicate the p-type or n-type properties of the conductor, respectively. Here, pristine SWCNT films showed a p-type nature through hole doping with water or oxygen and the Seebeck coefficient was positive (black in Fig. 2b). However, the Seebeck coefficient of the SWCNT films was negative after immersion in the solution, indicating that a n-type nature was generated by electron doping (red in Fig. 2b). In addition, the electrical conductivity of the SWCNT films increased from 1.9×10^4 S m^{-1} to 2.4×10^4 S m^{-1} after doping (Fig. 2c). This increase in the electrical conductivity originated from the increase in the carrier density.[4,15] In the ultraviolet-visible-near-infrared (UV-vis-NIR) absorption spectra of thin SWCNT films on a quartz substrate, the two broad peaks centred at 1040 nm and 1820 nm correspond to the S_{11} and S_{22} transitions of the semiconducting SWCNTs, which were bleached after doping (Fig. S2, ESI†). This result clearly indicates the effective doping of the SWCNT films. The Seebeck coefficient was unchanged when the SWCNT films were doped solely with the B_2pin_2 solution, or solely with the 4-CNpy solution (Fig. S3, ESI†).

We used scanning electron microscopy to examine the surface morphologies of the SWCNT films before and after doping (Fig. S4, ESI†). Random network and non-aggregation structures were observed in the non-doped and doped SWCNT films, respectively. This indicates that doping the 4-CNpy-boryl radical on the surface of the SWCNTs did not change their network morphology. The structural perspectives of the doped SWCNT films were evaluated using Raman spectroscopy.[14] The Raman bands of pristine SWCNTs at 1332 cm^{-1} (D band) and 1590 cm^{-1} (G band) originated from the sp^3 defects and the graphite-like structure of the SWCNTs, respectively (Fig. S5, ESI†). After doping, the G band of the doped SWCNT films shifted to 1584 cm^{-1}, indicating that electron doping occurred from the 4-CNpy-boryl radical to the SWCNTs. However, the D band intensity of the doped SWCNT films did not change compared to that of the pristine SWCNT film. This indicates that the defect density of the SWCNTs did not change after electron doping by the 4-CNpy-boryl radical.

X-ray photoelectron spectroscopy (XPS) is the powerful tool to characterize the chemical structure of the dopant molecules on the surface as well as the electronic state of the SWCNTs. Fig. 2 shows narrow XPS scans of the doped SWCNT films (for the survey scan, see Fig. S6, ESI†) for N 1s (Fig. 2d), C 1s (Fig. 2e) and B 1s (Fig. 2f). In the N 1s region, the peak was deconvoluted into two peaks centred at 400 and 402 eV (red line). Compared to the N 1s of 4-CNpy solely doped on SWCNTs (blue line), the peak at 400 eV was assigned to N 1s of a cyano group and a pyridine, whereas the new peak at 402 eV was assigned to quaternary pyridine.[16,17] The presence of the quaternary peak clearly indicates the coordination of 4-CNpy to B_2pin_2. In the C 1s peak, the doped SWCNT films shifted to a higher binding energy by 0.2 eV after doping (Fig. 2e), indicating that SWCNTs was n-doped and, consequently, the Fermi level was upshifted. However, in the B 1s peak, the doped SWCNT films showed a peak at 193 eV; no such peak was observed in the SWCNT films solely doped with B_2pin_2 prepared as the control. The absence of the B 1s peak for the control films indicates the sublimation of B_2pin_2 under ultra-high vacuum conditions (green line in Fig. 2f). This result indicates the dopant molecules formed by mixing of B_2pin_2 and 4-CNpy strongly interacted with SWCNT surface. From these XPS results, we concluded the formation of the dopant cation on the surface of SWCNT due to the electron transfer from 4-CNpy-boryl radical to SWCNTs, resulting in the n-doping of SWCNTs (Fig. 2a).

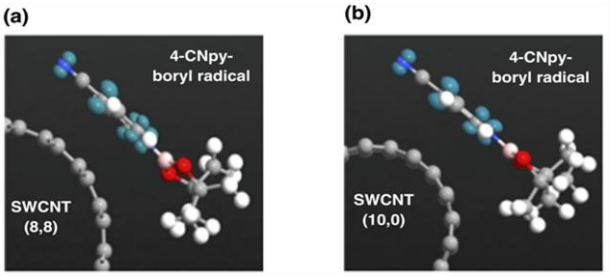

Fig. 3 Optimized geometries and the spin density distributions of SWCNT/4-CNpy-boryl radical complexes: (a) 4-CNpy-boryl radical/SWCNT (8,8) and (b) 4-CNpy-boryl radical/SWCNT (10,0). 4-CNpy-boryl radicals of the spin density are colored in iron blue. Boron, carbon, nitrogen and oxygen atoms are colored pink, gray, blue and red, respectively.

To further understand the SWCNT doping by the 4-CNpy-boryl radical, we performed density functional theory (DFT) calculations on the 4-CNpy-boryl radical on the surface of SWCNTs with chiral indices of (8,8) and (10,0), using Perdew-Burke-Ernzerhof (PBE) functional and numerical atomic orbitals (NAOs). The optimised geometries and spin density distributions of the SWCNT/4-CNpy-boryl radical complexes are summarised in Fig. 3. The dopant unit was aligned perpendicular to the SWCNT to avoid steric repulsion between the methyl groups of the dopant unit and the SWCNTs. Both the spin density distributions of the 4-CNpy-boryl radical show 0.7 e^-, which is lower than one electron density. This provided indirect evidence for electron transfer from the 4-CNpy-boryl radical. Furthermore, we performed Mulliken and Bader population analysis to understand the nature of the electron exchange between the SWCNTs and the 4-CNpy-boryl radical. The charge of the dopant unit in the complexes was 0.3 e^- and the shortest distances between SWCNT and 4-CNpy-radical were 3.35 Å for SWCNT (8,8) and 3.31 Å for SWCNT (10,0). These results suggest that a major electrostatic interaction occurred between the negatively charged SWCNTs and the positively charged dopant unit. The SOMO of the 4-CNpy-boryl radical was –4.03 eV at the UB3LYP/6-31G(d,p) level, which is higher than the conduction band of SWCNT (–4.2 eV)[13]. Thus, electron transfer from the radical to the SWCNTs is possible.

To study the effect of the captodative effect of the 4-CNpy-boryl radical on electron doping, we also prepared doped SWCNT films using 4-phenylpyridine (4-Phpy) and 4-methoxypyridine (4-OMepy) instead of 4-CNpy. The captodative effect of pyridine ligands was not expected to occur in the former two because of the electron-donating

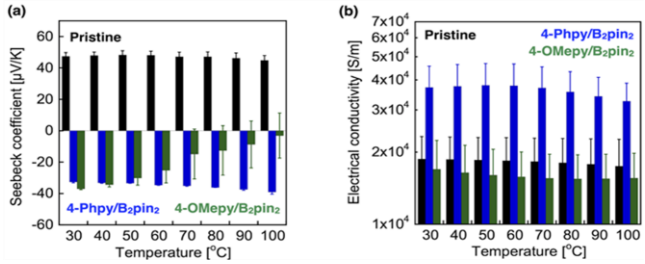

Fig. 4 Temperature dependence of (a) the Seebeck coefficient and (b) the electrical conductivities of pristine SWCNT (black), SWCNT films doped with 4-Phpy/B_2pin_2 (blue) and 4-OMepy/B_2pin_2 (green).

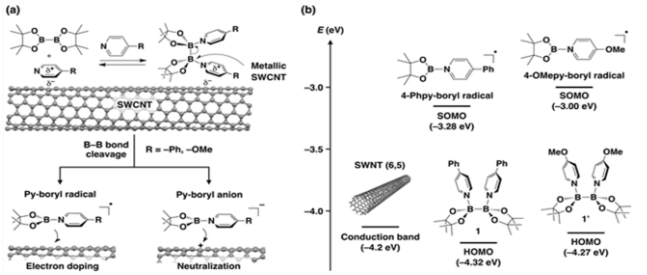

Fig. 5 (a) Plausible doping mechanism of B_2pin_2 with pyridines, followed by B–B bond cleavage of B_2pin_2on the surface of SWCNT. (b) Energy levels of **1**, **1'**, 4-Phpy-boryl radical and 4-OMepy-boryl radical.

natures of the Ph and OMe substitutions. In fact, Zhang and Jiao reported that 4-Phpy could not cleave the B–B bond of B_2pin_2 in the absence of a strong base.[18] However, it is interesting that here the Seebeck coefficients of SWCNT films doped with 4-Phpy/B_2pin_2 and 4-OMepy/B_2pin_2 solutions both showed a n-type nature, even though the ESR signals of these solutions were not observed (Fig. 4a and Fig. S1, ESI†). In addition, the electrical conductivities of the SWCNT films doped with the 4-Phpy/B_2pin_2 mixture increased from 1.9 × 10^4 S m^{-1} to 3.7 × 10^4 S m^{-1}, clearly indicating efficient electron doping (blue in Fig. 4b). Similarly, the SWCNT films doped with 4-OMepy/B_2pin_2 showed a n-type nature, but the Seebeck coefficients of these doped films became positive as the temperature increased (green dots in Fig. 4a). We recognized that the Seebeck coefficient of the SWCNT films doped by 4-Phpy/B_2pin_2 was relatively stable for a few days, while that of SWCNT films doped by 4-CNpy-boryl radical changed to p-type nature after 24 hours (Fig. S9, ESI†).

XPS analysis of the SWCNT films doped with 4-Phpy/B_2pin_2 and 4-OMepy/B_2pin_2 clearly revealed the presence of the B 1s peak and the shift of the C 1s peak (Figs. S7 and S8, ESI†), as observed for the SWCNT films doped by the 4-CNpy-boryl radical. For the N 1s peak, however, a broad peak ranging from 398 to 404 eV was observed for the films doped with 4-Phpy/B_2pin_2 and 4-OMepy/B_2pin_2 mixtures, as well as for the films doped solely with 4-Phpy and 4-OMepy. We thus interpreted that the 4-Phpy and 4-OMepy moieties were weakly positively charged on the SWCNTs' surfaces due to the electron-donating nature of 4-Ph and 4-OMe. Thereafter, sp^3–sp^3 diboranes (**1** and **1'**) were formed by the reaction of B_2pin_2 with positively charged pyridines. Heterotic cleavage of the B-B bond might have generated py-boryl radicals and py-boryl anions through electron transfer from metallic SWCNTs via the SWCNT network to **1** and **1'**. As a result, the radicals could have acted as electron reagents for SWCNTs, while the anions could have neutralised the positively charged SWCNTs through electron transfer (Fig. 5a). The highest occupied molecular orbitals (HOMO) of **1** was calculated to be –4.32 eV at the B3LYP/6-31G(d,p) level, which was not energetically favourable to electron transfer to the conduction band of SWCNT (–4.2 eV) (Fig. 5b). However, the SOMO of the 4-Phpy-boryl radical was –3.28 eV at the UB3LYP/6-31G(d,p) level, which is higher than the SOMO level of the 4-CNpy-boryl radical. Similarly, the HOMO of **1'** was –4.27 eV, which does not reach the conduction band of SWCNT, but the SOMO of the 4-OMepy-boryl radical was evaluated to be –3.00 eV (Fig.

5b). This result supports the formation of the py-boryl radicals on the surfaces of SWCNTs. The electron transfer to SWCNTs could have taken place effectively in these conditions.

However, the mass concentrations of boron estimated by XPS for the films doped with 4-Phpy- and 4-OMepy-boryl radicals were 1.03% and 0.44%, respectively, whereas the films doped with the 4-CNpy-boryl radical contained 1.45% boron. We assumed that the boron concentrations of the films doped with 4-OMepy-boryl radicals probably lower due to the destabilisation of the corresponding radicals by the electron donation effect from the methoxy group on the pyridine ring. Such instability may have caused the poor thermal stability of the film doped with the 4-OMepy-boryl radical (green in Fig. 4a). Therefore, the importance of the captodative effect of the py-boryl radical was clarified in this study.

In summary, we have demonstrated that the 4-CNpy-boryl radical can act as an electron-doping reagent for SWCNTs. Surface analysis of n-doped SWCNT films and theoretical calculations revealed that the doping mechanism comprised electron transfer from the SOMO of the 4-CNpy-boryl radical to the conduction band of the SWCNTs, where the captodative effect of the radicals and the formation of the py-boryl cations were both found to be essential for stable doping. The py-boryl radical may be useful not only as an electron dopant for SWCNTs, but also for organic and inorganic semiconductors by developing the molecular design of boryl radicals. Systematic investigations using various py-boryl radicals to study the doping mechanism as well to improve the air stability are currently undergoing and will be published in the future.

This work was supported by KAKENHI (No. 18H01816, 19K23633 and 20K15355) and bilateral programs (No. AJ190078) of the Japan Society for the Promotion of Science (JSPS) and the Nanotechnology Platform Project from the Ministry of Education, Culture, Sports, Science and Technology (MEXT), Japan, and Core Research for Evolutional Science and Technology (CREST) (No. AJ199002) from Japan Science and Technology Agency (JST), Japan.

Conflicts of interest

There are no conflicts to declare.

Notes and references

1 (a) E. Jouguelet, C. Mathis and P. Petit, *Chem. Phys. Lett.* 2000, **318**, 561; (b) J. Kong and H. Dai, *J. Phys. Chem. B* 2001, **105**, 2890; (c) L. Brownlie and J. Shapter, *Carbon* 2018, **126**, 257.

2 (a) L. Duclaux, *Carbon* 2002, **40**, 1751; (b) W. Zhou, J. Vavro, N. M. Nemes, J. E. Fischer, F. Borondics, K. Kamarás and D. B. Tanner, *Phys. Rev. B* 2005, **71**, 205423; (c) R. S. Lee, H. J. Kim, J. E. Fischer, A. Thess and R. E. Smalley, *Nature* 1997, **388**, 255.

3 T. Takenobu, T. Takano, M. Shiraishi, Y. Murakami, M. Ata, H. Kataura, Y. Achiba and Y. Iwasa, *Nat. Mater.* 2003, **2**, 683.

4 Y. Nonoguchi, K. Ohashi, R. Kanazawa, K. Ashiba, K. Hata, T. Nakagawa, C. Adachi, T. Tanase and T. Kawai, *Sci. Rep*., 2013, **3**.

5 Y.-F. Li, I.-S. Wong, T.-C. Lai, W. Chin and W.-K. Hsu, *Appl. Phys. Lett*. 2010, **97**, 153123.

6 M. Shim, A. Javey, N. W. S. Kam and H. Dai, *J. Am. Chem. Soc.* 2001, **123**, 11512.

7 (a) S. M. Kim, J. H. Jang, K. K. Kim, H. K. Park, J. J. Bae, W. J. Yu, I. H. Lee, G. Kim, D. D. Loc, U. J. Kim, E.-H. Lee, H.-J. Shin, J.-Y. Choi and Y. H. Lee, *J. Am. Chem. Soc*. 2009, **131**, 327; (b) C. Biswas, S. Y. Lee, T. H. Ly, A. Ghosh, Q. N. Dang and Y. H. Lee, *ACS Nano* 2011, **5**, 9817.

8 K. Funahashi, N. Tanaka, Y. Shoji, N. Imazu, K. Nakayama, K. Kanahashi, H. Shirae, S. Noda, H. Ohta, T. Fukushima and T. Takenobu, *Appl. Phys. Exp.* 2017, **10**, 035101.

9 (a) Y. Segawa, M. Yamashita and K. Nozaki, *Science* 2006, **314**, 113; (b) Y. Segawa, Y. Suzuki, M. Yamashita and K. Nozaki, *J. Am. Chem. Soc.* 2008, **130**, 16069.

10 (a) S. H. Ueng, A. Solovyev, X. Yuan, S. J. Geib, L. Fensterbank, E. Lacôte, M. Malacria, M. Newcomb, J. C. Walton and D. P. Curran, *J. Am. Chem. Soc*. 2009, **131**, 11256; (b) T. Matsumoto and F. P. Gabbaï, *Organometallics* 2009, **28**, 4252; (c) J. C. Walton, M. M. Brahmi, L. Fensterbank, E. Lacôte, M. Malacria, Q. Chu, S. H. Ueng, A. Solovyev and D. P. Curran, *J. Am. Chem. Soc*. 2010, **132**, 2350; (d) Y. Aramaki, H. Omiya, M. Yamashita, K. Nakabayashi, S. Ohkoshi and K. Nozaki, *J. Am. Chem. Soc.* 2012, **134**, 19989; (e) P. Bissinger, H. Braunschweig, A. Damme, I. Krummenacher, A. K. Phukan, K. Radacki, S. Sugawara, *Angew. Chem. Int. Ed.* 2014, **53**, 7360; (f) D. Lu, C. Wu and P. Li, *Chem. Eur. J.* 2014, **20**, 1630; (g) F. Dahcheh, D. Martin, D. W. Stephan and G. Bertrand, *Angew. Chem. Int. Ed*. 2014, **53**, 13159; (h) A. J. Rosenthal, M. Devillard, K. Miqueu, G. Bouhadir and D. Bourissou, *Angew. Chem. Int. Ed.* 2015, **54**, 9198; (i) M. F. S. Valverde, P. Schweyen, D. Gisinger, T. Ban-nenberg, M. Freytag, C. Kleeberg and M. Tamm, *Angew. Chem. Int. Ed.* 2017, **56**, 1135.

11 G. Wang, H. Zhang, J. Zhao, W. Li, J. Cao, C. Zhu and S. Li, *Angew. Chem. Int. Ed.* 2016, **55**, 5985.

12 L. Stella, *Acc. Chem. Res.* 1985, **18**, 148.

13 (a) Y. Nakashima, N. Nakashima and T. Fujigaya, *Synth. Met.* 2017, **225**, 76; (b) Y. Nakashima, R. Yamaguchi, F. Toshimitsu, M. Matsumoto, A. Borah, A. Staykov, M. Saidul Islam, S. Hayami and T. Fujigaya, *ACS Appl. Nano Mater.* 2019, **2**, 4703.

14 X. Mao, Z. Li, Y. Liu, X. Nie, B. Li, Q. Jiang, C. Gao, Y. Gao and L. Wang, *Chem. Eng. J.*, 2021, **405**, 126616.

15 Y. Nonoguchi, M. Nakano, T. Murayama, H. Hagino, S. Hama, K. Miyazaki, R. Matsubara, M. Nakamura and T. Kawai, *Adv. Funct. Mater.* 2016, **26**, 3021.

16 See examples: (a) X. Yang, J. Li, J. Liu, Y. Tian, B. Li, K. Cao, S. Liu, M. Hou, S. Li and L. Ma, *J. Mater. Chem. A*, 2014, **2**, 1550; (b) K. Müller, J. C. Moreno-López, S. Gottardi, U. Meinhardt, H. Yildirim, A. Kara, M. Kivala and M. Stöhr, *Chem. Eur. J.* 2016, **22**, 581; (c) Z. Kong, Q. Wang and L. Ding *Appl. Surf. Sci.* 2009, **256**, 1372; (d) F. Tao, W. S. Sim, G. Q. Xu and M. H. Qiao, *J. Am. Chem. Soc.* 2001**, 123***,* 9397.

17 See examples: (a) M. K. Kuntumallaa, M. Attrasha, R. Akhvlediania, S. Michaelsona and A. Hoffmana, *Appl. Surf. Sci.* 2020, **525**, 146562; (b) A. S. Jombert, M. K. Bayazit, K. S. Coleman and D. A. Zeze, *ChemNanoMat* 2015, **1**, 353; (c) S. Men, D. S. Mitchell, K. R. J. Lovelock and Peter Licence, *ChemPhysChem* 2015, **16**, 2211; (d) E. T. Kang and K. G. Neoh, *Mol. Phys.* 1990, **70**, 1057.

18 L. Zhang and L. Jiao, *Chem. Sci.* 2018, **9**, 2711.